Chemistry Research Journal, 2022, 7(5):73-92

Available online www.chemrj.org

Research Article

ISSN: 2455-8990
CODEN(USA): CRJHA5

Quantum Mechanical Depictions of Chemical Bonding and Structural Stability of Tri–hydrated Bisulfate Cluster $[HSO_4(H_2O)_3]^-$

Anant Babu Marahatta*[,1, 2]

[1]Department of Chemistry, Amrit Science Campus, Tribhuvan University, Kathmandu, Nepal
[2]Engineering Chemistry and Applied Science Research Unit, Kathford Int'l College of Engineering and Management (Affiliated to Tribhuvan University), Kathford Int'l Education and Research Foundation, Lalitpur, Nepal
*Corresponding author *(e-mail): abmarahatta@gmail.com*

Abstract The inexistence of HSO_4^- radical practically in isolated forms but high prevalence in dissimilar sized hydrated clusters $[HSO_4^-(H_2O)_{n\,=\,1–16}]$ have gained substantial attentions towards understanding nucleation growth mechanisms of the marine and atmospheric aerosols, molecular-level interactions of the ionic/acidic solvation, and chaotropic type ionic affinity for sequential hydration. Interestingly, the most prevailing yet intriguing facts behind this hydration, *viz.* (a) stabilizing effect of the negative charge reduces quickly whenever $n > 3$, (b) binding thermodynamics (strength) of HSO_4^- & H_2O decreases (increases) with increasing n ($n \leq 4$); reflect that the $[HSO_4^-(H_2O)_3]$ form is the biggest bisulfate cluster having mostly the highest structural and energetic stabilities. These typical characteristic features of the size-selected hydrated bisulfate clusters motivate the work reported here, in which chemical bonding & structural stabilities of the $[HSO_4(H_2O)_3]^-$ cluster are interpreted through the electronic wavefunction based molecular orbitals (MOs) approaches as they depict them *via* stereographic views of the electron density rather sticking to the position of the atomic nuclei in the 3D space. The total molecular electron density surface & its complete contour mapping, and the explicitly extracted MOs iso-surfaces & their individual contour diagrams are used here to grant the quantum mechanical insights into the orbital interactions, atomic bonding, molecular stabilities with a closed 3D structural topology, and the realistic electronic structure of the specific atoms & bonds with probabilistic electron amplitudes for the $[HSO_4(H_2O)_3]^-$ specimen. In support of this, the Mulliken revealed asymmetric electronic population and irregular trend of the Mulliken charges distribution in it are also presented.

Keywords MOs Approaches, Tri-hydrated Bisulfate Cluster, Contour Plot, Bonding Analysis

1. Introduction

The Sulphur-centered large singly charged HSO_4^- ions are one of the most prevalently found anionic species with wide range percentage abundancies [1]. In the atmosphere, they exist as quite trivial tropospheric ions with few potential roles in secondary aerosols formation process through the complex conglomeration of natural and

anthropogenic particulates [2]. They are actually regarded as the primary scatterers & absorbers of the solar radiation, and the most prominent condensation nuclei for the cloud formation [3, 4]. In the biological systems, they are recognized as quite essential denaturing agents more especially for the native structure of α-chymotrypsin [5]. In the marine systems, the relatively high abundance of them in sea water is confirmed which may cause the osmosis process of the distillation desalination method slower [6]. In the electrochemical systems such as lead acid battery and redox flow battery technologies, the ample quantity of them are present: the former uses 0.05M to 6.0M H_2SO_4 (aq.) [7, 8] while the latter uses inorganic sulfate compounds dissolved in a relatively dilute H_2SO_4 (aq.) [9–11] as their working electrolytes. Even in the day-to-day balanced diets and nutrient enriched meals, and in various other samples of ordinary edible plants & their seeds, basic foods, drugs, and dog urine, a picomolar (10^{-12} *mol./l*) amount of them are detected [12,13]. The main reason behind these ubiquities and predominant existence in such mineral-enriched aqueous systems is because of their chaotropic properties; a weak yet significant preference of the HSO_4^- ions towards undergoing sequential hydration, ion-induced nucleation [14–22], and interfering hydrogen bonding of the water network.

Since the inexistence of HSO_4^- ions practically in isolated forms but high prevalence in dissimilar sized hydrated forms ($[HSO_4^-(H_2O)_n]$; n (hydration number) = 1–16 are already confirmed through the experimental (IR & MS spectroscopies) and theoretical/computational (basin-hoping *Monte Carlo*) [14] techniques, the *ab initio* based quantum mechanical computations are still very needful in order to reveal more reliable and quantitative explanations required for ensuring their existence more especially in the low hydration states ($n \leq 3$). This is because from the very beginning, the quantum mechanical means have been recognizing as the relatively more crucial and trustworthy tools for examining structural, energetic, and thermodynamic stability (instability) of the microhydrated (unhydrated) clusters of the kosmotropic and chaotropic ions whose internally existing intramolecular type Coulombic interactions must be addressed mathematically [15]. In regard to this, present author has employed DFT based quantum mechanical method and reported the concerned electronic structures & stabilities, and the QSPR predicted electronic properties of the microhydrated SO_4^{2-} (kosmotropic) and HSO_4^- (chaotropic) ions (n = 1–16) elsewhere [16–22] where structural entity of them and the related electronic properties are confirmed quantitatively. However, the way of depicting chemical bonding and structural entity of the microhydrated ionic clusters just by examining positions of their atomic nuclei in the 3D space is relatively less quantitative than the electron density based molecular orbitals (hereafter, MOs) approaches. To the knowledge of this author, the prospective research papers concentrating on the MOs and electron/charge density analytical approaches for disclosing quantitative perspectives of the geometrical stabilities of $[HSO_4(H_2O)_{n \leq 3}]^-$ clusters are rarely available. Herein, the molecular wavefunctions $\Psi(x,t)$ based quantum mechanical insights into the orbital interactions, electron/charge density distributions, atomic bonding, 3D structural stabilities, and inter-particle interactions between the HSO_4^- and solvating H_2O of one of the low energy hydrated clusters of the bisulfate ion, *viz.* $[HSO_4(H_2O)_3]^-$ are presented. The main reasons behind the selection of $[HSO_4(H_2O)_3]^-$ specimen here are due to the following well-established yet quite intriguing fact of HSO_4^- hydration: (a) the stabilizing effect of negative charge reduces quickly whenever $n > 3$ [2, 22], (b) the binding thermodynamics of HSO_4^-/H_2O decreases with increasing n, (c) $[HSO_4(H_2O)_n]^-$ moieties are more readily formed and strongly bound to each other whenever $n \leq 4$. Kurten *et al.* [23] and Husar *et al.* [2] confirmed the same characteristic features while studying the affinity of H_2O molecules towards HSO_4^- ions through "MP2 with correction for higher-order electron correlation" and "CCSD(T) RI–MP2" methods respectively. More importantly, the latter authors reported thermodynamically favored hydrated HSO_4^- clusters even at the moderate tropospheric conditions: (a) at T ≤ 298.15 K & relative humidity RH = 20%, smaller clusters with $n \leq 3$ $[HSO_4(H_2O)_{n=1-3}]^-$ are relatively more stable while (b) at T ≤ 273.15 K & RH > 20%, bigger clusters with $n \geq 4$ $[HSO_4(H_2O)_{n=4-6}]^-$ are stable. However, the formation of the bisulfate hydrated clusters at the lower atmosphere is argued as kinetically limited due to the small number concentration of HSO_4^- ions ($[HSO_4^-] \cong 10^2 - 10^3$ cm^{-3}) [24].

Being the MOs: (a) solutions of the Schrodinger wave mechanical equation, (b) molecular wavefunctions $\Psi(x,t)$ representing sum of the products of individual molecular orbitals $\Psi_i(x,t)$, (c) electrons' most-probable sites, and (d) building blocks for describing electron density distribution over the entire molecular surface, the MOs approaches of bonding analyses are realized as the better quantitative mean for interpreting precise electronic structures/ delocalizations including positions and energies of the electrons in molecules [25]. Since energy of the electrons in a molecule is quantized, $\Psi(x,t)$ governs not only the dynamic behavior of all the electrons in the definite (allowed) energy levels but also describes the manner in which electronic charge is three dimensionally disseminated. Unfortunately, $\Psi(x,t)$ itself doesn't have any physical significance. Nevertheless, it's squared $\Psi^2(x,t)$ which is proportional to probability of finding the electrons in an infinitesimal volume at a given point of space and time is very useful to quantize electron density distribution or simply the electron density $\rho(x,y,z)$ over the entire molecular surface [26, 27]. Actually, the MOs' electron density $\Psi^2(x,t)$ representing stereoscopic display of the total molecular electron density surface (hereafter, TMEDS) is a 3D cloud of the negative charge distributing non-uniformly in density throughout the molecule and hence, serves as a fundamental yet precise basis of examining chemical bonding and equilibrium molecular geometry [27]. Additionally, the MOs' iso-surfaces and contour plots facilitate chemists to understand: (a) what is actually happening to the electron density while attaining structural stability, (b) variation of the charge density throughout the molecule, (c) 3D characters of the MOs, and (d) shape and spatial extent of the MOs. Typically, the former is connection of those set of points in the 3D space that have the same numerical values of $\Psi(x,t)$ (for the electron density), and the latter is simply the sketch of the contour lines joining all those points [24–27]. As a whole, the complete information of the chemical bonds & their characterizations, atomic/interatomic surface interactions, rigorous distributions of the electron cloud along each internuclear axis, and the quantum mechanical overviews for illuminating the existence of hydrated molecular motifs with closed 3D structural topology etc. can be obtained from the TMEDS, individual MOs' iso-surfaces and contour plots [24–29]. In support of these MOs interpretations, the Mulliken population analyses [30] with charge density plots stand as the most computationally cheap yet semi-quantitative mean for exploring how actually the electronic charges associated with each MOs, atomic orbitals AOs, and atomic centers are disseminated throughout the molecular specimens. In quantum mechanics, both of these analyses are routinely carried out through the LCAO MO based quantum mechanical models [31, 32] such as DFT; an LCAO-Kohn-Sham ansatz based mathematical scheme [33, 34]. In the current study, the same theoretical method with B3LYP type hybrid electron density functional and 6−31G (*d*, *p*) basis sets is applied to $[HSO_4(H_2O)_3]^-$ motif, and implemented both MOs and Mulliken population analytical approaches computationally for assessing all of its structural, atomic bonding, specific electronic and bonding interactions related quantum mechanical issues. The structure of this paper is organized as follows: the computational details are outlined in Methodological section, the specific results are presented in Results and Discussions section, and the concise summary is given in Conclusion section.

2. Computational Details

The *GaussView*: Gaussian graphical interface [35] was used to construct the trial molecular model of the tri-hydrated bisulfate cluster $[HSO_4(H_2O)_3]^-$. Among its two energetically different experimentally determined structural isomers reported elsewhere [36], the one showing good structural agreement with the low energy isomer was designed here computationally (Figure 1). During the stepwise peripheral addition of three molecule equivalent of H_2O to the central HSO_4^- unit, no inter-water and inter-water-bisulfate hydrogen bonds were allowed to develop. The 3D positions/orientations of each atomic nuclei of each H_2O molecule were determined based on the bond vibrations spectral analyses of the microhydrated bisulfate anions with $n \leq 9$ (the Gas-phase infrared multiple photon dissociation (IRMPD) and harmonic MP2/6−311+G (*d*, *p*) stick spectra are available elsewhere [15]) and fixed them accordingly. The Cartesian coordinates of thus modeled tri-hydrated molecular entity were extracted explicitly and the energy minimization calculations were run at first through computationally low cost, low level *ab initio* based quantum mechanical method (HF/STO−3G). The HF/STO−3G converged molecular geometry (Cartesian

coordinates) was then taken as an input (trial) structure for the relatively high computational cost, high level hybrid functional DFT method with 6−31G (*d, p*) level basis sets. The split-valence double-zeta mathematical function "6−31G" was actually chosen here to incorporate both core and valence orbitals of each atom, and the polarization mathematical functions in parentheses "(*d, p*)" were selected just to evaluate the degrees of bond polarity of each and every chemical bonds. The *Gaussian 09* electronic structures calculation package [37] was used to implement DFT: B3LYP/ 6−31G (*d, p*) method computationally. The specific *Gaussian* keyword *%chk* was chosen so as to generate the concerned *.chk* file in the working directory, which was later converted to *Gaussview* readable *.fchk* format through the *formchk* module of the same package for visualizing electron density based MOs & their iso-surfaces and the specific contour diagrams in the 3D space. The integral values of the ionic charge and spin multiplicity = 2*S*+1; *S* (total spin) = *n*/2 were specified as (*−1, 1*) in the format of (*charge, spin multiplicity*). The self-consistent-field (hereafter, SCF) with both default SCF procedures; SCF=Tight and Berny algorithm for geometry optimizations to a local minimum were selected while routing the script to the way of getting iterative solutions of the Schrodinger wave mechanical equations. Accordingly, all the concerned Gaussian keywords instructed in the manual available elsewhere [38, 39] were used as per the needs of the current mathematical computations. After a successful termination of the energy minimization calculations, all the structural interpretations were performed with the advanced computer graphics aided molecular visualization and manipulation tools *viz. GaussView*, *Jmol*, and *Molden*. Additionally, all the formatted *.fchk* files were accessed through the *GaussView*, and the entire chemical bonds related quantitative information was extracted from the 3D stereographic sketches of the TMEDS, MOs' iso-surfaces, and their respective contour plots. The standard set of the |isovalue|: MO = 0.0200, Density = 0.0004 was used to display them separately in the 3D plot axis. For the Mulliken population analysis, all the Mulliken derived partial atomic charges were extracted from the DFT generated *.log* files, and analyzed their intensive distribution trends throughout the $[HSO_4(H_2O)_3]^-$specimen by drawing Mulliken atomic charges (hereafter, MAC) plot.

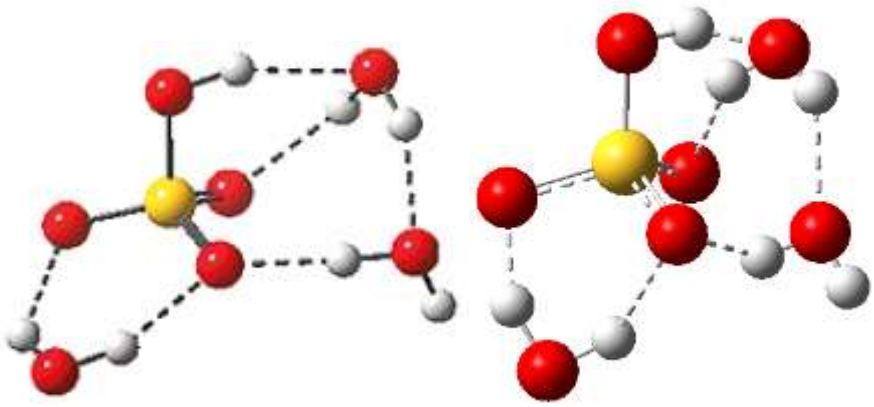

Figure 1: (a) An experimental IRMPD determined structure of low energy isomer reproduced from ref. 15; and (b) A GaussView sketched trial molecular model; of the tri-hydrated bisulfate cluster $[HSO_4(H_2O)_3]^-$. The DFT produced equilibrium structure of the same model in different spatial atomic orientations is displayed in Figure 2(a).

3. Results and Discussions

3.1. Quantitative Perspectives of the Chemical Bonding

In general, the atoms while forming diatomic or multi-atomic chemical compounds always try to reach into the lowest-energy state. The only way for them to attain this naturally allowed *energy state is to share their own valence*

electrons either to each other or to another bonding atoms. Such electron pairs shared on the verge of forming chemical bonds are termed as bonding electron pairs as they are mostly recognized as strong atomic binding force that gives utmost strength to the chemical compounds. Such type of force actually arises as a result of the symmetric or asymmetric electronic distributions throughout the bonding homo or hetero atoms, and provides a substantial potentiality to hold them tightly in a chemical compound is known as covalent type chemical bond. In fact, the same is the reason why the theoretical chemists/physicists have been intensifying their attentions to the chemical bonds from the very beginning more especially for the sake of acquiring quantum mechanical information of the chemical bonds, interpreting molecular structures through the delocalized 3D electron density surfaces, and deriving most closely associated molecular wavefunction $\Psi(x,t)$ based geometrical descriptors of the covalently bonded molecular compounds. Before realizing wave nature of the electrons and formulating the same probabilistic matter wave in the form of Schrodinger wave mechanical equation, the two different electronic theories of covalent bond *viz.* Lewis and Valence Shell Electron Pair Repulsion VSEPR were prevailed mainly as the principal means of determining 3D configuration of the bonding and non-bonding electron pairs around the central atom which in turn leads to the approximation of typical molecular geometry/shape with the concerned geometrical descriptors such as bond angles, bond lengths, dihedral angles etc. Similarly, the next quite prevailing theory *viz.* Valence Bond Theory VBT was also adopted in general chemistry as a relatively more realistic mean of determining molecular geometry and addressing the extraordinary strength of the covalent bonds. The major differences between the explanations/interpretations bestowed by these electronic theories lie on their basic assumptions: the former two consider distribution of the bonding and non-bonding (lone) electrons (particle nature) around the central atom as key-points in determining molecular geometry while the latter makes 3D orientations of the hybridized atomic orbitals AOs of the central atom holding the same type electron pairs as its fundamental basis. Accordingly, the first two theories never consider exceptionally high strength of the covalent bond as their major concern but the latter one significantly addresses it through the orbital approaches: the extent to which two atomic orbitals of the participating atoms overlap to each other prior to sharing bonding electron pairs between themselves always determines the strength of the covalent bond. Nevertheless, the adverse lacking parts of all these theories are to accept electrons as the localized particles and to look attentively at the electronic configuration of the atoms as a primary part of the covalent bonds. The quantum mechanical theories (hereafter, QMT) based on the LCAO approximations, however, attempt to theorize electrons' behavior as probabilistic matter wave and, hence undertake the electronic distributions in atoms and the entire molecular geometry through molecular wavefunction $\Psi(x,t)$ based Schrodinger equations and symmetry of the AOs respectively [40]. More specifically, all the QMTs critically treat bonding and non-bonding electrons as probabilistic matter waves with wavelength λ *via* the Schrodinger wave mechanical model, and incorporate the effect of two or more than two nuclei in the delocalized electron cloud of the MOs whose spatial distribution is seriously taken as an essential mean of evaluating both distorted and regular type molecular geometries precisely [41]. Therefore, all the Schrodinger wave equation based QMTs are regarded as the most appropriate quantitative theoretical means of illuminating thermodynamic, energetic, and kinetic perspectives of the chemical bonds and the molecular stability.

As stated in section 1, the QMTs not only tend to describe energy and position of the electrons at a given point of space x and time t with literal solutions of the Schrödinger wave mechanical equation but also to speculate quantitative distribution of the electron density $\rho(x,y,z)$ over the entire MOs/molecular surfaces. And, the complete chemical bond with 3D molecular structures related quantum mechanical information are derived from the squared of the molecular wavefunction $\Psi^2(x,t)$. But, the major hurdle faced by the theoretical chemists is to extract all the $\Psi(x,t)$ encoded information related to bonding electrons & their interactions with substantial contributions to the atomic binding force in molecules [42]. Towards resolving this, none of the computational tools are recognized so far as fully able theoretical means. Despite suffering from these notable criticisms, few quantum mechanical ways that are categorized into following four different analytical approaches are still accepted as indispensable and implementable type computational means just for assessing the complete solution of the Schrödinger wave

mechanical equation: (a) Electron density analysis, (b) Energy analysis, (c) MOs analysis, and (d) Population analysis [42– 44]. Herein, the last two means are employed and accessed DFT: B3LYP/6−31G (*d*, *p*) generated electronic information of the chemical bonds including electron density surfaces of each and every MOs and their iso-surfaces of the specifically selected tri-hydrated bisulfate $[HSO_4(H_2O)_3]^-$ cluster computationally. Beside this, they are employed here to enlighten the significance of molecular wavefunction based delocalized MOs and electron density based interatomic bonding interactions in elucidating structural and bonding stability of the hydrated motifs by referring $[HSO_4(H_2O)_3]^-$ ion. Actually, this type of the quantum mechanical investigations are well recognized among the chemists as indispensable theoretical means mainly for disclosing few underlying facts behind the extra stability of low hydrated ionic entities as several sophisticated experimental tools and techniques are still incapable of deriving same level explanations with precise 3D quantitative pictorial views. The concerned theoretical results and discussions that are in closed connection with the MOs analyses of the preferentially selected low hydrated bisulfate cluster $[HSO_4(H_2O)_3]^-$ are presented below concisely yet comprehensively.

3.1.1 Molecular Orbitals (MOs) Analysis

As per the well-established LCAO statement "the number of MOs (Ψ) formed are always equal to that of the intermixing AOs (Ψ_i) of the bonding atoms" [42], the mathematical technique involved in it for computing bonding and non-bonding MOs is none other than the superposition of the AOs. This basic principle of constructing MOs simply by the quantum superposition of the AOs with progression of energy from the lowest to the highest in fact leads to molecular orbitals energy level diagram: a sketch of the energetically organized MOs (energy levels) on the basis of which the trend of setting up new MOs from the AOs can be qualitatively explored. Beside this, the chemists mainly contemplated this diagram in describing (a) ascending/descending order of the energy levels, (b) why some complicated molecular compounds have unique bond order, (c) where the chemical bonds (bonding electron pairs) are centralized in them, (d) where the nuclei of the intermixing AOs are located in the resulting MOs, and sometimes in correcting very first guessed molecular geometry as well. In spite of these compliments, the MOs energy level diagrams are not frequently used due to their inability in demonstrating realistic views of the chemical bonding, in visualizing 3D distribution of the electron cloud & in sketching closely associated electron density based molecular structures in the 3D space, and they never allow the chemists for the quantitative prediction/estimation of the electronic energy during real-time computations of the MOs. This is why, both delocalized electron density iso-surfaces & their contour plots and total molecular electron density surface of the MOs involved in building up concerned MO diagrams collectively are very needful. In real-time computations, they can only be produced through the quantum mechanical computational packages designed to perform complex mathematical procedures. The LCAO based density functional mathematical scheme with B3LYP functional run under the *Gaussian 09* package is one of such computational means that has an exceptional potentiality in approximating exchange-correlation energy functional.

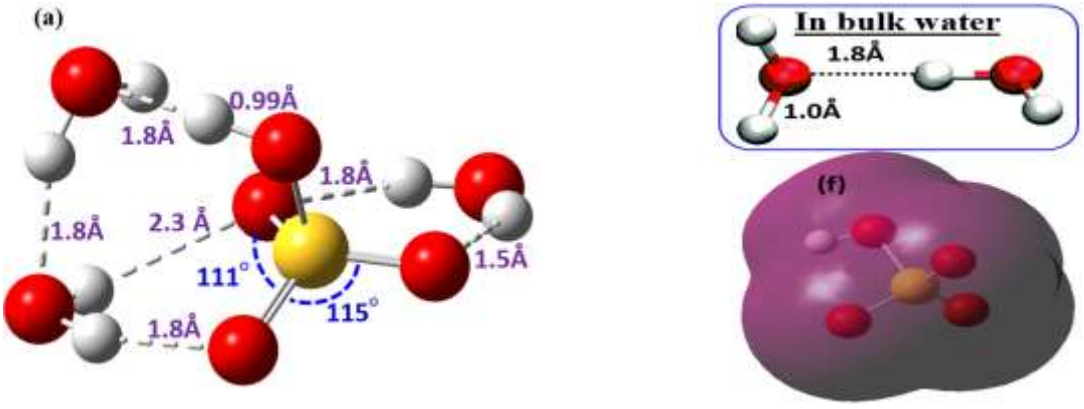

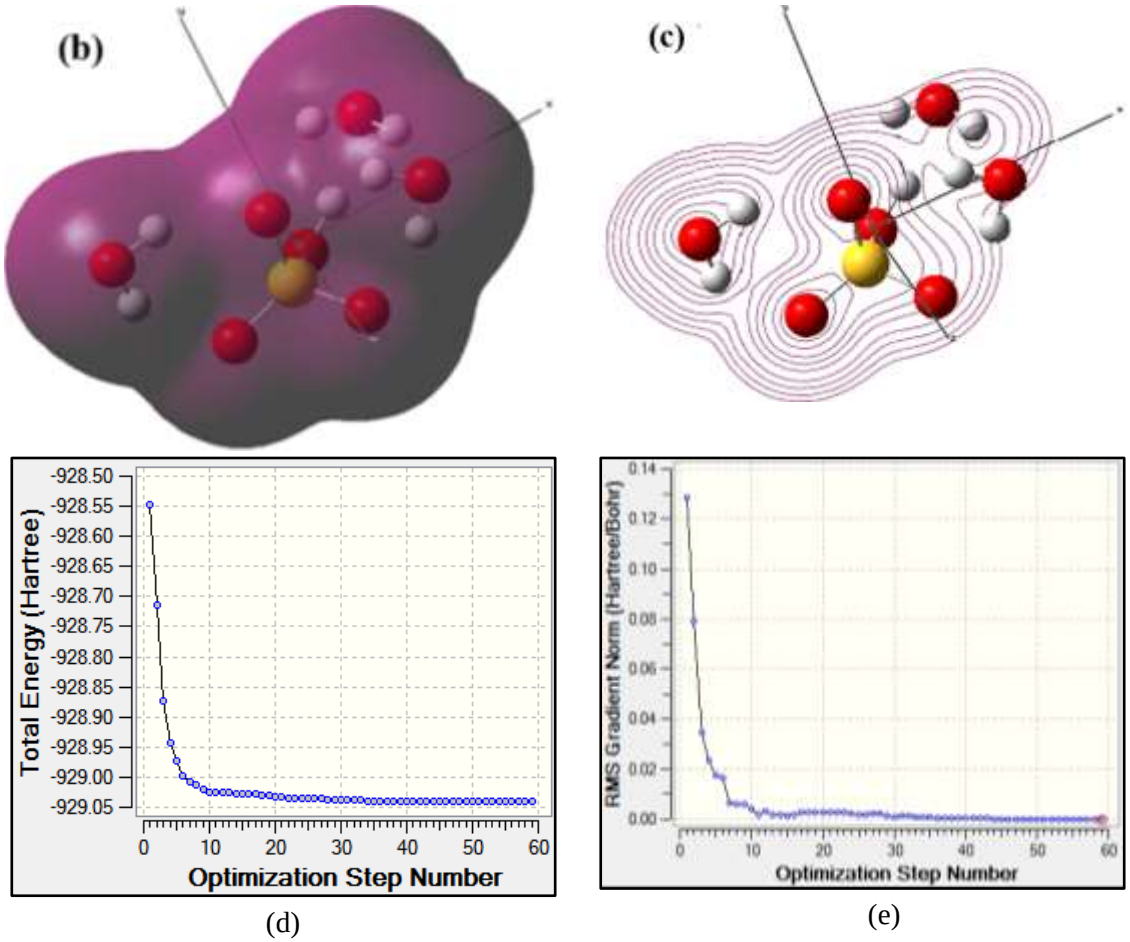

Figure 2: The DFT derived (a) ground state electronic structure, (b)/(c) total electron density surface (TEDS)/contour lines (transparent mode) at an |isovalue|: MO = 0.0200, Density = 0.0004 from Total SCF density, (d)/(e) change in total electronic energy/RMS gradient with optimization step numbers, of $[HSO_4(H_2O)_3]^-$ ion. The individual completely fulfilled bonding MOs/contours that build up (b)/(c) are shown in Figure 2. Just for reference, the similar type TEDS for an unhydrated HSO_4^- ion is shown in (f).

Herein, the DFT: B3LYP/ 6−31G (*d*, *p*) produced 3D total molecular electron density surface of $[HSO_4(H_2O)_3]^-$ ion and its individual sets of the MOs iso-surfaces & their respective contour plots displayed in Figure 2 and Figure 3 respectively are used to reveal the most realistic views of its chemical bonding and molecular stability. The former type delocalized surface & contour plot, and the latter type iso-surfaces & their contour lines of the selected bonding MOs are shown in Figure 2(b) and Figure 3 respectively. The 3D surface displayed in Figure 2(b) was actually a complete compilation form of the electron density iso-surfaces of all the bonding and non-bonding MOs including those listed in Figure 3. It remains as a quantitative tool to quantize the outermost boundaries of the electron density distributed three dimensionally around each and every specific nuclei of the $[HSO_4(H_2O)_3]^-$ ion. Additionally, it depicts not only the electrons' most probable sites located in the vicinity of the atomic nuclei of $[HSO_4(H_2O)_3]^-$ but also high electron density slots lying on their effective bonding regions. Similarly, it identifies the polar type chemical bonds of $[HSO_4(H_2O)_3]^-$; the covalent bonds with relatively massive (poor) electron dense regions towards the more electronegative (electropositive) atomic nuclei are generally categorized as polar type chemical bonds. Since the degree of polarity of the chemical bonds arises as a result of the electro-attractive forces exerted by the

more electronegative atoms (they pull the bonding electron pairs towards themselves creating partial positive charge on their bonding atoms), their presence in $[HSO_4(H_2O)_3]^-$ has been confirmed by identifying both electronic protruded and electronic depleted regions appeared on the DFT derived total electron density surface (Figure 2(b)). All these typical yet convenient electronic features of the total molecular electron density surface ultimately underscore that the $[HSO_4(H_2O)_3]^-$ ion exists in the form of low energy stable hydrated molecular entity with a definite 3D electronic structure leading towards the confirmation of its following supplementary yet needy molecular properties: (a) fixed molecular boundary, (b) closed 3D geometry, (c) definite molecular shapes & sizes, (d) symmetrical and asymmetrical electronic clouds distributed throughout all the specific atomic nuclei, (e) precise molecular boundaries in the 3D space, (f) discrete electrophilic and nucleophilic attacking regions (electron rich and electron deficient regions respectively), (g) specific atomic terminals with high and low electronegative regions, (h) polar type covalent bond, (i) most probable steric, electrostatic, and orbital interactions sites, (j) significant steric, electrostatic, and orbital contributions to the ground state electronic energy, (k) distorted and delocalized electron cloud etc. In conclusion, the total electron density surface of $[HSO_4(H_2O)_3]^-$ with clearly visible distinguished electronic protrusions maps its definite 3D molecular shape along with presenting a precise structural orientation of the centrally located HSO_4^- unit inbound to the three peripheral H_2O molecules, further highlighting the existence of stable and rigid type hydrogen bonded structural motif of $[HSO_4(H_2O)_3]^-$ in the wide ranged aqueous systems.

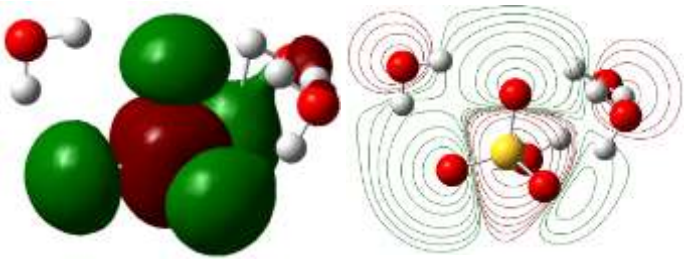

(1) 20a MO and contours, $E = -0.47239$ *a.u.*

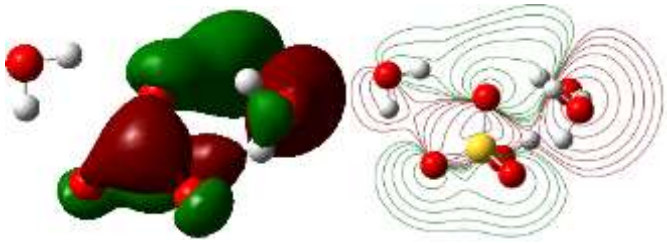

(2) 21a MO and contours, $E = -0.38227$ *a.u.*

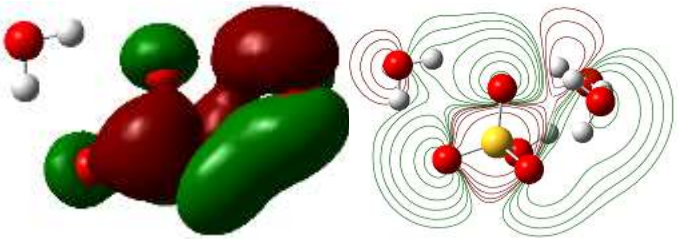

(3) 22a MO and contours, $E = -0.38076$ *a.u.*

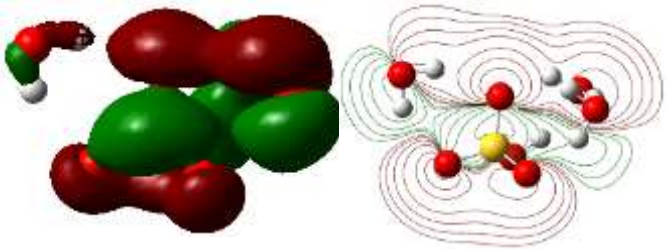

(4) 23a MO and contours, $E = -0.37538$ *a.u.*

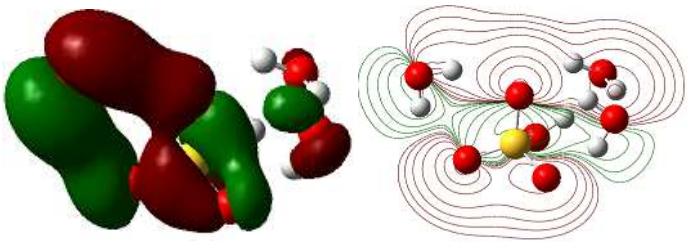

(5) 24a MO and contours, $E = -0.34126$ *a.u*

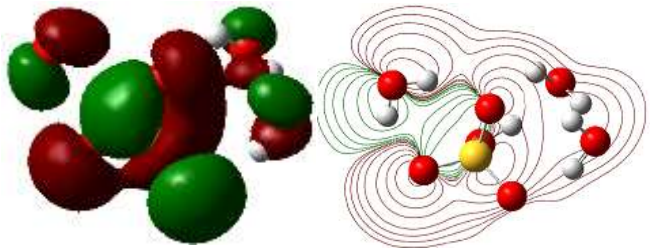

(6) 25a MO and contours, $E = -0.31941$ *a.u.*

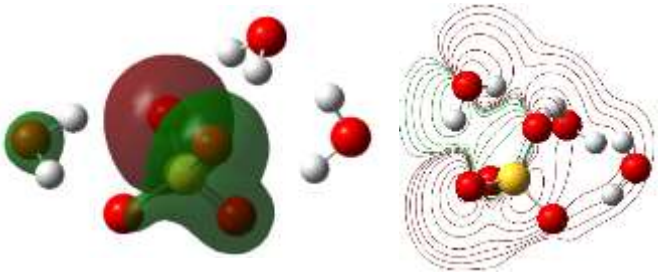

(7) 26a MO and contours, $E = -0.31693$ *a.u.*

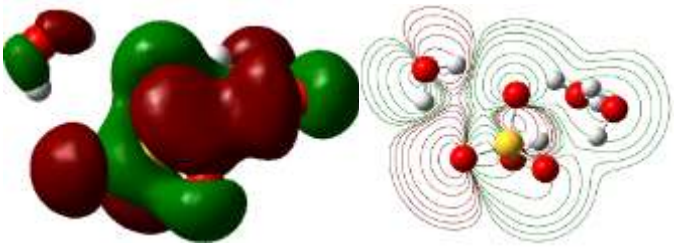

(8) 27a MO and contours, $E = -0.27817$ *a.u.*

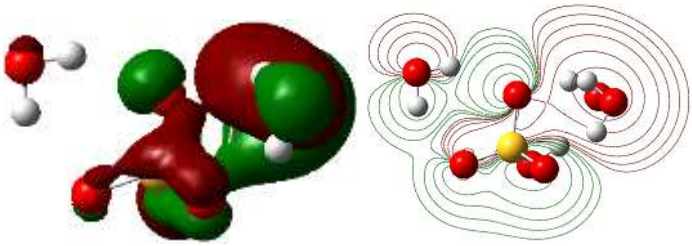

(9) 28a MO and contours, $E = -0.26764$ *a.u.*

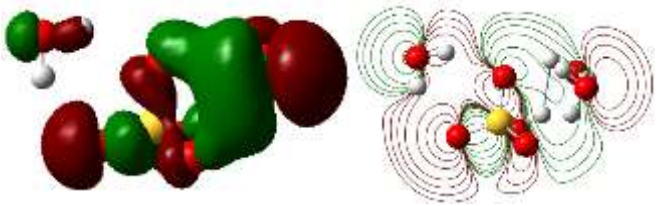

(10) 29a MO and contours, $E = -0.26689$ *a.u.*

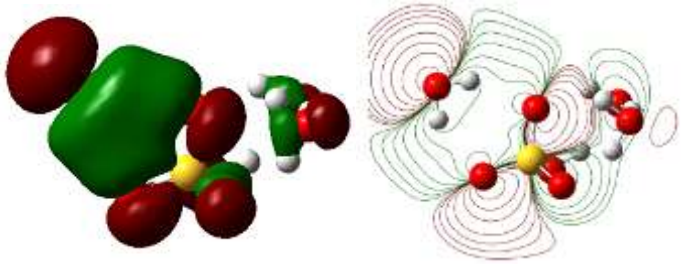

(11) 30a MO and contours, $E = -0.23013$ *a.u.*

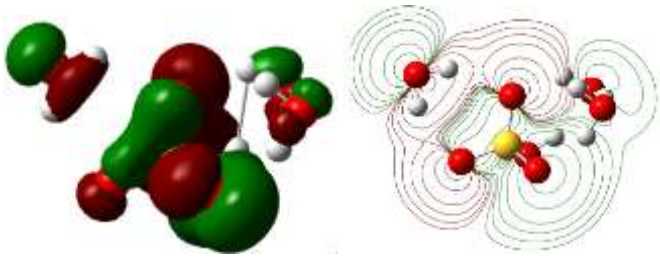

(12) 31a MO and contours, $E = -0.20725$ *a.u.*

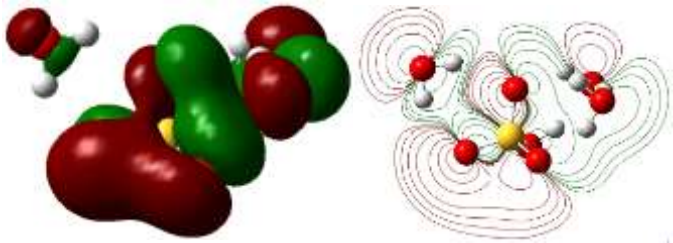

(13) 32a MO and contours, E = −0.19046 *a. u.*

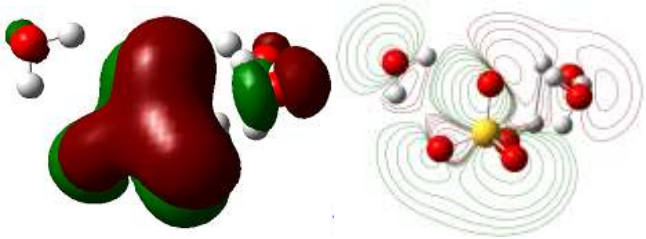

(14) 33a MO and contours, E = −0.18429 *a.u.*

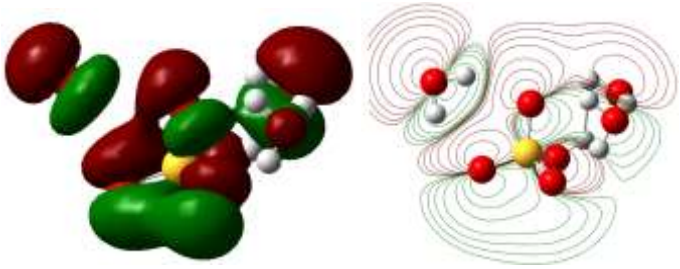

(15) 34a MO and contours, E = − 0.17987 *a.u.*

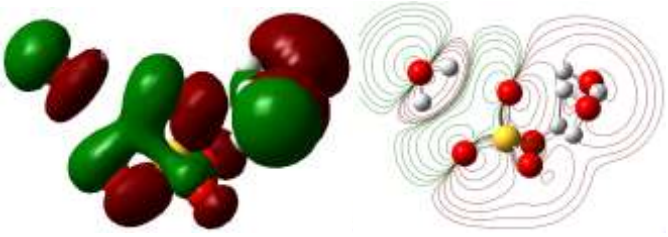

(16) 35a MO and contours, E = − 0.17228 *a.u.*

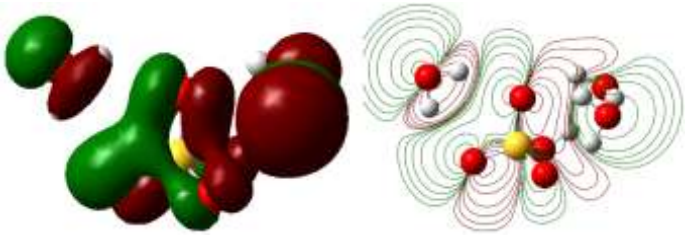

(17) 36a MO and contours, E = − 0.17101 *a.u.*

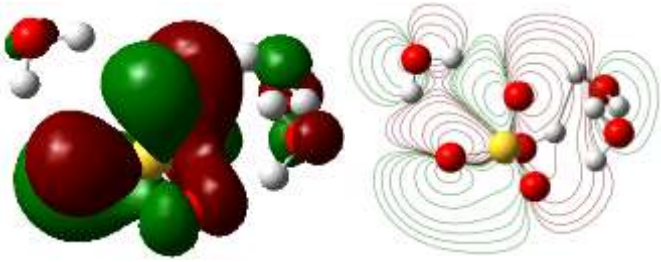

(18) 37a MO and contours, E = – 0.14613 *a.u.*

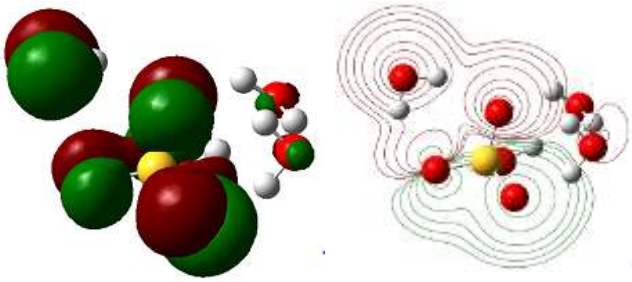

(19) 38a MO and contours, E = – 0.13120 *a.u.*

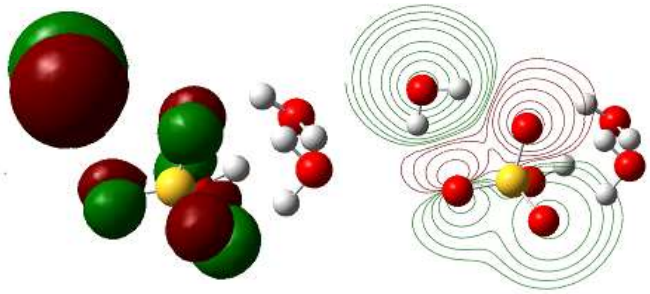

(20) 39a HOMO–1 and contours, E = – 0.12520 *a.u.*

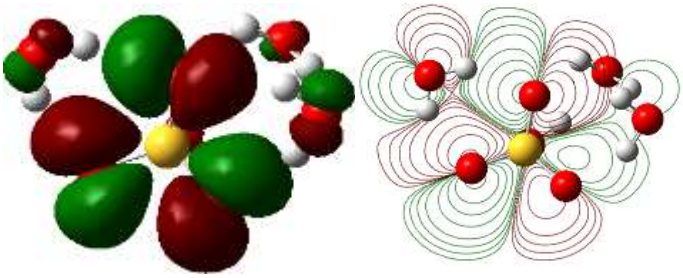

(21) 40a HOMO and contours, *E* = – 0.11851 *a.u.*

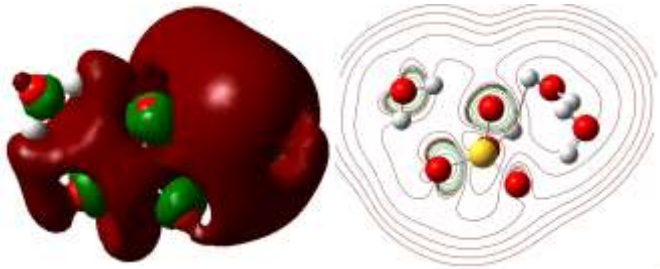

(22) 41a LUMO and contours, *E* = +0.20273 *a.u.*

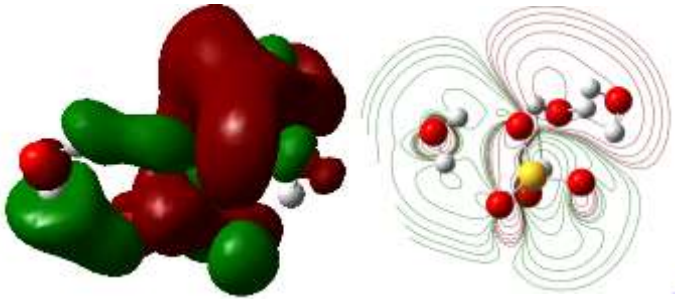

(23) 42a LUMO+1 and contours, *E* = +0.24429 *a.u.*

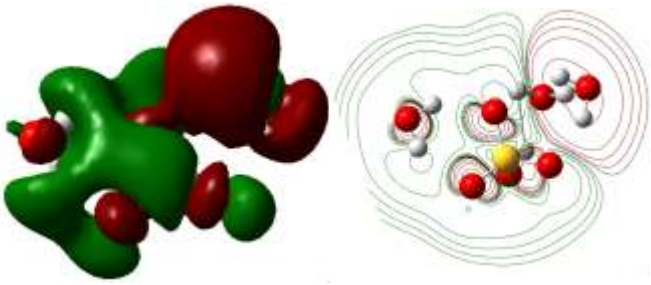

(24) 43a LUMO+2 and contours, *E* = +0.26490 *a.u.*

Figure 3: The DFT computed real MOs (completely full-filled 20a–40a MOs) and contours of $[HSO_4(H_2O)_3]^-$ ion at an |isovalue|: MO = 0.0200, Density = 0.0004. These MOs/contours collectively construct the major part of the total electron density surface (TEDS) displayed in Figure 1(b)/(c). The core MOs 1a–19a comprising very negligible electron cloud, and contributing significantly less to the TEDS are excluded here. The HOMO–1, HOMO, LUMO, LUMO+1, and LUMO+2 are also displayed here for critical bonding analyses.

In the support of the same, the DFT:B3LYP/6−31G (*d, p*) converged ground state equilibrium electronic structure of $[HSO_4(H_2O)_3]^-$ (Figure 2(a)) and all the associated geometrical/structural descriptors measured in the positions of the concerned atomic nuclei bestowed quite relevant yet qualitative type evidences as reported by the same author elsewhere [20]. More importantly, the validity of the H_2O-linked hydrogen bonds to the central HSO_4^- unit (Figure 2(a); hydrogen bond length = 1.8 Å) is justified by the experimentally and theoretically determined hydrogen bond length of the water network (as shown in the inset of Figure 2). Just for the reference, the DFT: B3LYP/6−31G (*d, p*) derived total molecular electron density surface of the unhydrated HSO_4^- ion is also shown in Figure 2(f) whose significant yet distinguished electronic protrusions confirm that even at the unhydrated state, HSO_4^- ion possesses polar type covalent bonds.

Since the total electronic energy and the root mean squared (RMS) gradient are the most significant mathematical indicators for inspecting whether the convergence analysis/energy minimization calculations of the $[HSO_4(H_2O)_3]^-$ are being run smoothly or not, the graphical plots demonstrating the variations of these parameters with the optimization step numbers are shown in Figure 2(d) and Figure 2(e) respectively. While observing them closely, no any processing of the abnormal mathematical terminations during the entire quantum mechanical convergence procedures was observed. Such a smoothly expanding graphical drawing indeed givebacks the essential proofs of undergoing significant inter particle interactions between the constituents of $[HSO_4(H_2O)_3]^-$: the central HSO_4^- unit does interact with the three molecule equivalent of peripheral H_2O molecules while attaining energetically and

thermodynamically most stable structural motif. The normal termination of these graphical sketches eventually speculates that the $[HSO_4(H_2O)_3]^-$ ion does stabilize itself as a single, isolated, entangled, and low hydrated structural entity form.

While the symmetric and/or antisymmetric distributions of the electron cloud in $[HSO_4(H_2O)_3]^-$ were visualized and quantized through the thorough analyses of the 3D total molecular electron density surface, they are still inappropriate and inapplicable in deriving in-depth yet quantitative and realistic insights into the chemical bonds and the specific type electronic distributions in particular type bond formation process. This is why, the 3D electron density iso-surfaces of each and every MOs of $[HSO_4(H_2O)_3]^-$ are needful here. In addition to this, each and every iso-surfaces are treated here as the most significant theoretical means of interpreting all types of the chemical bonds and their most probable electronic interactions in $[HSO_4(H_2O)_3]^-$. In this study, they are preferentially selected and utilized here mainly for exploring the quantum mechanical information related to whether the electron density is atom-centered, localized/ delocalized at the specific bonding sites, and concentrated into the specific atomic proximity or not. Additionally, the contour plots of every MOs representing electron density slices passing through the entire molecular entity are also referred here just for strengthening the structural/ geometrical predictions made through the MOs' iso-surfaces. Actually, both of these quantum mechanical means (Figure 3) are the magnified 3D stereoscopic image sketched through the graphics hardware and chemistry software. They collectively permit chemists in understanding real-time, full-color, 3D electronic distributions of each set of the bonding MOs (including frontier MOs) that are designated as the real MOs due to having a paired electron with opposite spins. The core MOs **1a-19a** of the $[HSO_4(H_2O)_3]^-$ ion that are practically recognized as less contributing MOs to the total electron density surface due to having a significantly less electronic distributions around the specific bonds are selectively excluded here, as well as nonbonding MOs. The DFT: B3LYP/6−31G (*d*, *p*) derived Eigen value (E) in atomic unit (*a. u.*; Hartree E_h), and a set of the iso-surface values |isovalue|: MO = 0.0200 *a. u.*, Density = 0.0004 *a. u.* (1 *a. u.* = 6.748 $e/Å^3$) used for generating density surfaces and contour plots for the rest of the bonding MOs (**20a-41a**) and the LUMO + 1 and LUMO + 2 orbitals are mentioned in the respective captions (Figure 3). Since all the 3D electron density surfaces generated through these specifically selected dimensions of the |isovalue| set are recognized as consistent mean as kinetic theory data [45, 46], these surfaces derived for the $[HSO_4(H_2O)_3]^-$ ion can be realized as the most precise yet visible van der Waals' envelope of the molecules that enables us in theorizing its very real views of the three dimensionally distributed electron clouds and thereby approximates an ultimate geometrical shape.

Even though the LCAO approach needs AOs intermixing coefficients c_i between the different wavefunctions ψ (for e.g., in the SP^3 mixing, the wavefunctions $\psi_{SP3}$is of the form: $\psi_{SP3}(r) = c_1\psi_{2s}(r) + c_2\psi_{2p_x}(r) + c_3\psi_{2p_y}(r) + c_4\psi_{2p_z}(r)$), they were not determined here due to their inaccessibility in explaining structural stability of the $[HSO_4(H_2O)_3]^-$ as the present electron density based analytical methods accept natural bond order (NBO) analysis as a non-mandatory mean. After all, each and every MOs' electron density surfaces and the respective contour lines of them present unambiguous views of the molecular symmetry property and the dense electronic cloud delocalized over the entire molecular surface of the tri-hydrated structural motif $[HSO_4(H_2O)_3]^-$. Similarly, all these delocalized type MOs' electron density surfaces deduce the fact that all the electrons occupying molecular orbitals of $[HSO_4(H_2O)_3]^-$ are spreading throughout the entire molecular region, and the bonding & non-bonding electrons in it are not confined only to the vicinity of one or two atomic nuclei as assumed by the valence bond theory of covalent bonding but are propagated through all the bonding nuclei. Beside this, they imprecise the spatial distribution of the electrons throughout the molecule which in turn describes the particular regions in space where the valence electrons are most probably resided. More specifically, each of these electron density surfaces yields in-depth views of the delocalized electron cloud along with exhibiting how actually the MOs are constructed while the quantum computations are on the fly. In fact, the orbital interactions that take place between two or more that two AOs are the main cause of building up such delocalized type MOs whose electron density is observed as a propagated electron

cloud over the entire nuclear region of the $[HSO_4(H_2O)_3]^-$ as observed in Figure 3. All these comprehensive quantum mechanical descriptions not only provide the absolute image of the 3D molecular structure of this tri-hydrated bisulfate unit but also stand firmly as a good theoretical evidence for confirming the existence of its stable structural motif in the wide ranged aqueous and humid atmospheric systems. Furthermore, the completely closed envelope of the contour lines (Figure 3) of each MO of $[HSO_4(H_2O)_3]^-$ estimates its electron amplitudes that measure how far the electronic wave is departed from its average value [45]. As can be seen in each plot, these lines are spreading over the entire molecular surface of $[HSO_4(H_2O)_3]^-$ and approximating the boundaries inside which the dense electron cloud is localized. Apart from this, the electron density distribution in a plane containing all the nuclei of $[HSO_4(H_2O)_3]^-$, the density distribution around each of its atomic nuclei, and the profile of its density distribution along each internuclear axis are also mapped three dimensionally. Just like in all the succeeding contour diagrams that are being used in the standard quantum chemistry text books, the atomic unit values of each and every contours of all the MOs displayed in Figure 3 are assigned here in ascending order (in magnitude) from the outermost to the innermost one (towards the nuclei). So, they also enable us in mapping mainly the bond density differences in $[HSO_4 (H_2 O)_3]^-$ [45, 46]. As a whole, the DFT: B3LYP/6−31G (*d*, *p*) derived total electron density surfaces and iso-surfaces with contour plots of each and every MOs of $[HSO_4(H_2O)_3]^-$ quantitatively confirm its stable structural entity with significant orbital & atomic bonding interactions, highly polarized type covalent bonds, delocalized type MOs, propagated type electron cloud, definite van der Waals envelope, fixed electron boundaries, specific electron amplitudes, and the particular type electronic/van der Waals interactions. Towards revealing all these quantum mechanical perspectives for the sake of claiming the existence of tri-hydrated form of HSO_4^- $[HSO_4(H_2O)_3]^-$ in a single stable molecular entity, two well established traditional electronic theories of the covalent bonding viz. VSEPR and VBT are not recommended as good candidates as they treat both bonding/nonbonding electron pairs as particle nature and assume all the covalent bonds as localized electron pairs.

3.2 Mulliken Charge Density Plots and Population Analysis

In theoretical chemistry, the Mulliken population analysis: a wave function based population analysis method; is regarded as a "simply the best" method where some arbitrary and orbital based mathematical schemes are used in partitioning molecular wave functions computationally [31]. This theoretical technique is mainly employed here for deriving partial atomic charges of $[HSO_4(H_2O)_3]^-$ and their specific assignment to each of its individual atoms quantum mechanically as the total and individual electron density surfaces and their 3D stereographic mappings presented above in section 3.1 are still not recognized as the most appropriate computational means of providing quantitative data sets and the related numeral indices of the atomic charges. One of the main reasons why this method constitutes the most frequent choice among the theoretical chemists is due to its post-processing type computational procedure where a substantial focus is given to the local electron density. The same low-cost computing abilities actually make this method widely useful for predicting Mulliken partial atomic charges, electronic charges distribution, bond populations in the bulk materials, and sometimes even for the conformational analysis of the complex protein conveniently yet semi-quantitatively [31, 33]. Despite serious suffering from the basis set sensitivity of the Mulliken populations, its usefulness in elucidating oxidation states of the atoms, its inability to reproduce dipole moment, and its restriction in over-interpreting any observable properties of the atoms and molecules, it is repeatedly used quantum mechanical mean mainly for deriving satisfactory level mathematical data sets and the related numeral indices of the partial atomic charges as it always keeps the essential features same and maintains transferability and neutrality of the molecular systems well while the concerned computational calculations are on the fly [47, 48]. In fact, the Mulliken derived partial atomic charges are quite essential mainly to elucidate specific type atomic interactions involved in molecular compounds building up steps.

While the DFT procedure of executing Mulliken method is on the fly, the brief mathematical procedures, viz. (a) explicit division of the electron density $D_{\alpha\beta}$ and overlap matrix terms $S_{\alpha\beta}$ of the orbital occupation expression $\rho(r) = D_{\alpha\beta}S_{\alpha\beta}$, (b) entire summing up of all the populations of all the atomic orbitals on a single atom, and then

subtracting to the nuclear charge resulting a generation of the mathematical index on each atom (partial atomic charge) are fully incorporated. It further stresses that the Mulliken method implemented *via* the *Gaussian* run DFT algorithms usually attempt quantitative analyses of the local electron density of the molecular systems computationally.

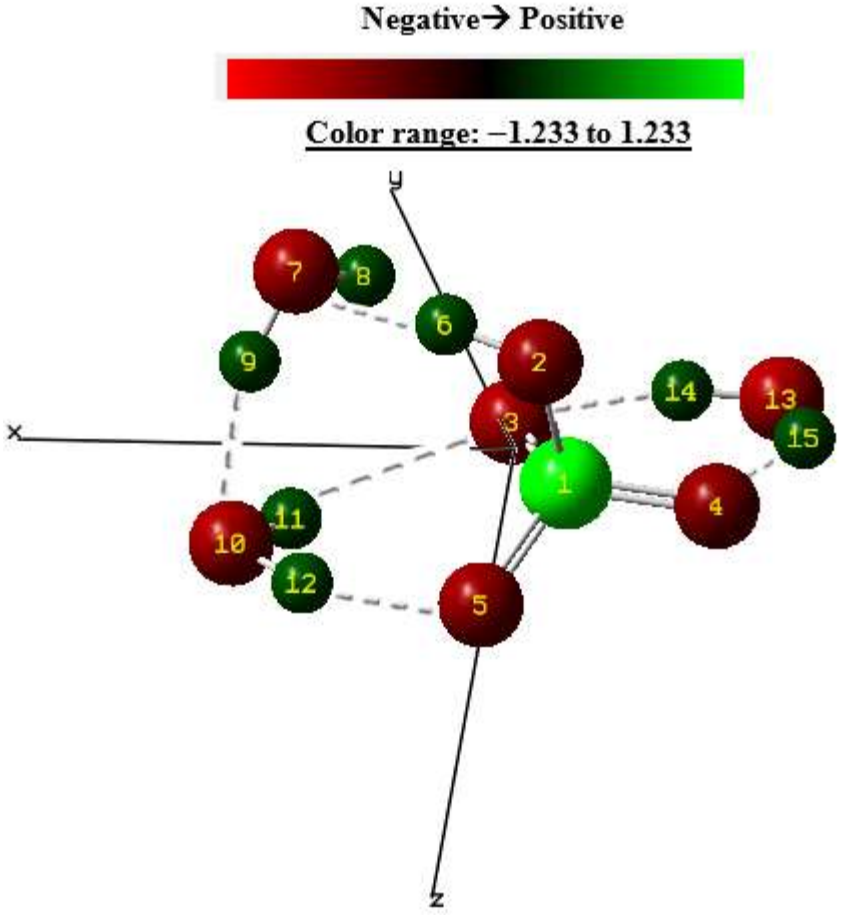

Figure 4: The Mulliken charges distribution in the DFT derived electronic structure of $[HSO_4(H_2O)_3]^-$. The symbols δ^+/δ^- on each atom indicate the deficiency/ sufficiency of electron density (polar type covalent bond). All the atoms are numbered as per the numeral labelling in Figure 1(a), and are colored by the intensity of the atomic charges. The color range and index are shown in the inset.

Therefore, the Mulliken predicted qualitative charge distributions and numeral charge indices of the atoms in the entire molecular specimen are also highly useful for approximating its most probable sites of electron density and for tracing out the degree of polarity of its covalent bonds. Additionally, almost all the Mulliken derived atomic charges are widely used explicitly as the force field calculations' effective computational parameters and the most significant mathematical descriptors for comparing/differentiating primary chemical properties of the two closely related molecular systems [31, 33]. Hence, the numeral indices of the partial atomic charges computed in this study are found as indispensable assets for explaining qualitative charge distributions in the entire $[HSO_4(H_2O)_3]^-$ specimen which indeed can be used successively as the supplementary data sets for supporting the underlying facts behind its existence in tri-hydrated moiety form in the wide ranged aqueous systems. As the absolute values of the Mulliken computed partial atomic charges are subjected to change with the minimal changes in the types of basis sets used, the numeral indices of the partial atomic charges (Table 1) of $[HSO_4(H_2O)_3]^-$ presented here are only

restricted to the underlying basis set of the type 6−31G (*d*, *p*). Herein, the same mathematical indices are used just to interpret some qualitative aspects of the irregular charge distributions, to produce information associated with the changes in electron density, and to get tentative idea about the degree of bond polarity in $[HSO_4(H_2O)_3]^-$.

Table 1: Mulliken derived atomic charges distribution in $[HSO_4(H_2O)_3]^-$ ion

Atom number	Atoms	Mulliken atomic charge (*a.u.*)
1	S	+1.292
2	O	–0.597
3	O	–0.644
4	O	–0.641
5	O	–0.642
6	H	+0.347
7	O	–0.409
8	H	+0.195
9	H	+0.234
10	O	–0.527
11	H	+0.262
12	H	+0.231
13	O	–0.736
14	H	+0.275
15	H	+0.360

Sum of the Mulliken atomic charges = –1.000 *a.u.* (It is exactly equal to the charge carried by $[HSO_4(H_2O)_3]^-$ specimen)

The explicitly derived partial atomic charges of the Sulphur (S), Hydrogen (H), and Oxygen (O) atoms of the $[HSO_4(H_2O)_3]^-$ ion are summarized in Table 1, where the atom numbers designated to each atom are in accordance with the atomic numerals assigned to each atom in Figure 3. In this stereographically displayed DFT: B3LYP/6−31G (*d*, *p*) derived low energy ground state electronic structure, each and every atoms are explicitly colored on the basis of the intensity of the distributions of these partial atomic charges with the prior fixing of the effective color index and range. In fact, the same color index is used here to identify the most negatively, most positively, and comparatively least positively charged atoms: the red colored spheroids (in central HSO_4^-: **O2**, **O3**, **O4**, and **O5**; in three peripheral H_2O: **O7**, **O10**, **O13**), the green colored spheroids (in central HSO_4^-: **S1**), and the dark green colored (in central HSO_4^-: **H6**, in three surrounding H_2O: **H8**, **H9**, **H11**, **H12**, **H14**, and **H15**) spheroids represent these irregular charge densities in $[HSO_4(H_2O)_3]^-$ respectively. Such inhomogeneously distributed Mulliken charges reflects that there is a presence of asymmetric electron density in each and every covalent bonds of the $[HSO_4(H_2O)_3]^-$ which in turn is closely associated with the resonating electron cloud delocalized over the central HSO_4^- unit as observed in the DFT produced low energy ground state electronic structures of the hydrated and unhydrated HSO_4^- ion (Figure 2). This irregular trend of the electronic distributions can be further generalized from the numeral values listed in Table 1, and their graphical sketch (Mulliken atomic charge (hereafter, MAC) plot) shown in Figure 5 where the first and last parts marked by the purple and blue colored rectangular boxes explain Mulliken charge distributions in the central HSO_4^- unit and in the centrally inbound peripheral H_2O molecules respectively. The MAC plot shows clearly that the central **S1** atom of the $HSO4^-$ unit has the most intense positive Mulliken charge as it hosts four electronegative **O** (**O2**, **O3**, **O4** and **O5**) atoms that have high tendency to attract the shared electron pairs towards themselves bearing almost an identical magnitude of the negative Mulliken charges (partial atomic charges) on each of them. Interestingly, the **O2** is observed as an atom with the lowest magnitude of the partial negative charges among its counterparts **O3**, **O4**, and **O5**. This is further due to its bonding connection (unlike **O3**, **O4**, and **O5** atoms) with the least electronegative **H6** atom designated + 0.347 *a. u.* magnitude of the

partial atomic charges. Accordingly, the **O** atoms of the three centrally inbound peripheral H_2O molecules, viz. **O7**, **O10**, and **O13** are found to have unequal magnitudes of the partial atomic charges. More specifically, the atom **O13** has the least negative charge among others. This might be due to its uninvolvement in hydrogen bond formation either with the central HSO_4^- unit or with the nearby H_2O molecules unlike **O7** and **O10** as illustrated by the DFT predicted low energy equilibrium structure and the Mulliken charge distribution figure shown in **Figure** 2(a) and Figure 4 respectively. The most important conclusion we can extract from this asymmetric type electronic distribution patterns is $[HSO_4(H_2O)_3]^-$ ion shows strong ability to hold all of its peripheral constituents together through the six different hydrogen bondings that are of course created in between partially negatively charged O atoms (**O3**, **O4**, and **O5**) of the central HSO_4^- unit and the more partially positively charged **H** atoms of the peripheral H_2O molecules (**H11**, **H12**, **H14**). In the meantime, the significantly higher ability of the oxygen (**O**) atom to attract a shared electron pair towards itself (electronegativity x^O = 3.44 in Pauling scale) than that for the Sulphur (x^S = 2.58 in Pauling scale) and Hydrogen (x^H = 2.20 in Pauling scale) atoms, and most importantly the three dimensional spatial distribution of the peripheral H_2O molecules illuminate the underlying facts behind the existence of intramolecular type hydrogen bonds (inter-particle hydrogen bonds) in tri-hydrated $[HSO_4(H_2O)_3]^-$ cluster, which in principle underscores the exceptional binding strength of the peripherally configured H_2O molecules between themselves and to the centrally located HSO_4^- unit (Figure 2(a)).

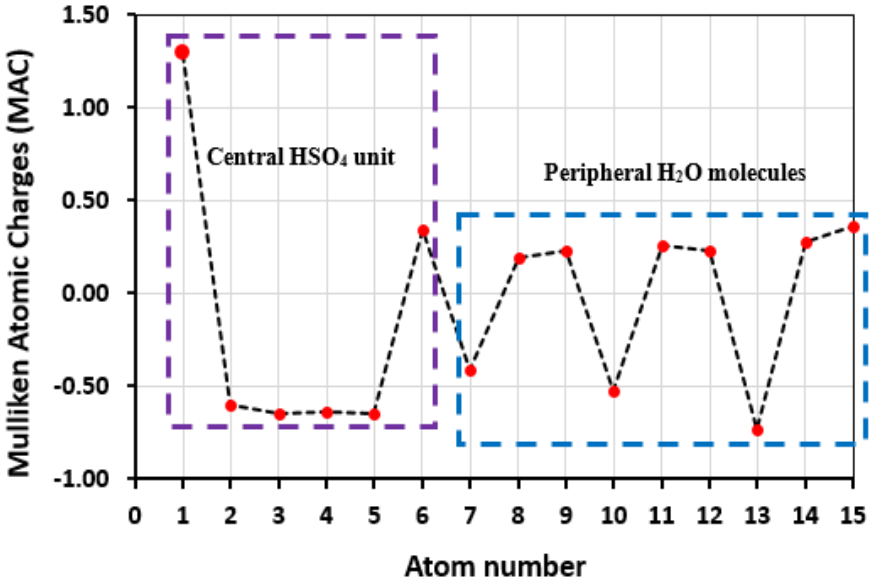

Figure 5: The Mulliken atomic charges (MAC) plot for $[HSO_4(H_2O)_3]^-$ ion computed under the DFT:B3LYP/6-31G(d,p) scheme. The purple and blue colored rectangular boxes mark the Mulliken charges distributions in the central HSO_4^- unit and in the centrally inbound peripheral H_2O molecules respectively

As a whole, the DFT: B3LYP/ 6−31G (*d, p*) derived Mulliken atomic charges and their disproportional distributions throughout the $[HSO_4(H_2O)_3]^-$ specimen have guaranteed the presence of either minimally polar or strongly polar chemical bonds in between more-electronegative (in this case **O**) and less-electronegative (in this case **H**) atoms which successively stands as a primary evidence behind the secrecy of attaining ionic stability even at a remarkably low hydration degree. If the fellow researchers are interested to investigate the same features of the hydrated ionic clusters with more quantitative means, present author recommends "CHELPG" (Charges from the Electrostatic Potential on Grid) charges as a good alternative to the Mulliken method as it computes more stable atom-centered charges that provides best fit to the molecular electrostatic potential and deduces the in-depth charge distributions in hetero-atomic molecular systems quantitatively [49, 50]. Similarly, present author also recommends Amsterdam Density Functional (ADF) scheme [51, 52]; one of the most emerging specific type DFT engines, as it is

mathematically formulated to compute partial atomic charges of the molecular systems without any strong sensitivities to the underlying basis sets.

4. Conclusion

The main objective of this research was to unveil the secrecy behind the structural/ geometrical, energetic, and thermodynamic stabilities of $[HSO_4(H_2O)_3]^-$ even at extremely low hydration state (n = 3). This smallest yet stable microhydrated bisulfate cluster is widely reported in the research papers as the ubiquitously available ionic species in several bisulfate and sulfate enriched day-to-day balanced diets and nutrient enriched meals, wide ranged aqueous chemical, physiological, biological, and electrochemical systems, and complex type atmospheric aerosols, marine ecosystems, and ocean technology. Towards acquiring the quantitative and decisive type information required to reveal the hidden facts behind its structural stability, the most potential quantum mechanical means, viz. wavefunction ($\Psi(x,t)$) based molecular orbitals (MOs) and Mulliken population analyses methods were adopted. The closely associated three dimensionally propagated electron density based geometrical descriptors such as chemical bonds, electronic structures & delocalizations including positions and energies of the electrons, bonding interactions among the atomic orbitals, electron amplitudes, van der Waals envelope, and the electron boundaries for the $[HSO_4(H_2O)_3]^-$ specimen were directly accessed through the routinely run LCAO-Kohn-Sham ansatz based DFT scheme with underlying hybrid density B3LYP functional and 6-31G (*d*, *p*) type complete basis sets. While assessing the relative significance of them in deducing these issues, all the required three dimensional stereographic views of the total molecular electron density surface (TMEDS) & its complete contours, and each & every occupied MOs' & their iso-surfaces with the concerned contour mappings of the specified ionic specimen were computed separately. One of the reasons why the DFT scheme became the first choice for this specific study is to integrate minimal yet pivotal type inter-particle interactions exist in between HSO_4^- and the three equivalent peripherally distributed H_2O molecules (between themselves as well) without which no accurate computation of the ground state electronic structure and the quantitative evaluation of the three dimensionally distributed electron cloud in $[HSO_4(H_2O)_3]^-$ can be achieved.

In this study, the DFT: B3LYP/6-31G (*d*, *p*) derived TMEDS approximated the closed three dimensional shape of the $[HSO_4(H_2O)_3]^-$ hydrated moiety with the disproportionate electronic distributions around its specific atomic nuclei. And, the clearly distinguishable and outward projected electronic protrusions appeared on the TMEDS confirmed the most probable locations of three hydrogen-bonded peripheral H_2O molecules that were set while constructing the 3D structural hydrated network with the central HSO_4^- unit. Similarly, the consistent explanations of the resonating electron cloud delocalized over the $[HSO_4(H_2O)_3]^-$ specimen granted by the DFT derived electron density iso-surfaces of its each occupied MOs confirmed that there is a direct involvement of orbital type bonding interactions between the two dissimilar type atoms in MOs' construction process. Accordingly, the most rigorous sites of finding its valence electrons in the 3D space were also roughly estimated. Apart from this, the 3D contour lines of each and every occupied MOs demonstrated how far its electronic wave is departed from the average (amplitudes of the electrons). In conclusion, all these quantum mechanical means predicted quite relevant and meticulous information that stands as a concise and comprehensive clarification behind declaring the existence of chemically bonded and energetically stable structural entity of $[HSO_4(H_2O)_3]^-$ in aqueous type systems. Besides this, the Mulliken revealed asymmetric electronic population and the irregular trend of atomic charges distribution became quite supportive mathematical datasets especially for quantifying specific type bonding interactions between the participating atomic orbitals.

5. Notes

The author declares no competing financial and non-financial conflicts of interests.

6. Acknowledgement

A small part of this work was carried out through the high-performance computing systems available at Cyberscience Center-Tohoku University, Sendai, Japan. The author is thankful to the entire editorial and reviewer board members for their constructive reviews.

References

[1]. J. Mähler, I. Persson, "A study of the hydration of the alkali metal ions in aqueous solution", *Inorganic Chemistry*, Vol. 51, Issue 1, pp. 425−438, 2011.

[2]. D. E. Husar, B. Temelso, A. L. Ashworth, G. C. Shields, "Hydration of the Bisulfate Ion: Atmospheric Implications", *Journal of Physical Chemistry A*, Vol. 16, pp. 5151−5163, 2012.

[3]. J. P. D. Abbatt, S. Benz, D. J. Cziczo, Z. Kanji, U. Lohmann, O. Möhler, "Solid Ammonium Sulfate Aerosols as Ice Nuclei: A Pathway for Cirrus Cloud Formation", *Science*, Vol. 313, Issue 5794, pp. 1770−1773, 2006.

[4]. J. Flahaut, M. Massé, L. Le Deit, P.Thollot, J.P. Bibring, F. Poulet, C. Quantin, N. Mangold, J. Michalski, J. L. Bishop, "Sulfate-rich deposits on mars: a review of their occurrences and geochemical implications", *Eighth International Conference on Mars*, 2014.

[5]. A. Kumar, A. Rani, P. Venkatesu, "A comparative study of the effects of the Hofmeister series anions of the ionic salts and ionic liquids on the stability of α-chymotrypsin", *New Journal of Chemistry*, Vol. 39, Issue 2, pp. 938−952, 2015.

[6]. B. B. Tanganov, "About sizes of the hydrated salt ions – the components of sea water", *Europian Journal of Natural History*, Vol. 1, pp. 36−37, 2013.

[7]. D. Pavlov, "*Lead Acid Batteries: Science and Technology*", Elsevier publisher, 2011.

[8]. D. Pavlov, A. Kirchev, M. Stoycheva, B. Monahov, "Influence of H_2SO_4 concentration on the mechanism of the processes and on the electrochemical activity of the $Pb/PbO_2/PbSO_4$ electrode", *Journal of Power Sources*, Vol. 137, Issue 2, pp. 288−308, 2004.

[9]. T. Yamamura, A. B. Marahatta, S. Yoshida and N. Tanno, "Vanadium Redox Cell", WIPO (PCT) Patent WO2016158295A1, 2016.

[10]. T. Yamamura, A. B. Marahatta, S. Yoshida and N. Tanno, "Vanadium Redox Flow Battery" Japan Patent JP2016189318A, 2016.

[11]. A. B. Marahatta, "Towards Understanding the Stabilities of Hydrated Vanadium (V) Complex Ions and the Pathway of V_2O_5 Precipitation in Catholyte Solution of Vanadium Redox Flow Battery", *International Journal of Progressive Sciences and Technologies*, Vol. 20, No. 2, pp. 348−364, 2020.

[12]. "Sodium Sulfate Functions in Daily Life–Formula–Uses" *https://azchemistry.com/ sodium-sulfate-function*

[13]. C. H. VanEtten, H. L. Tookey, "*Effects of Poisonous Plants on Livestock"*, Academic press, 1978.

[14]. R. R. Nair, M. Raju, S. Bhai, I. H. Raval, S. Haldar, B. Ganguly, P. B. Chatterjee, "Estimation of bisulfate in edible plant foods, dog urine, and drugs: picomolar level detection and bio-imaging in living organisms", *Analyst*, Vol. 144, pp. 5724−5737, 2019.

[15]. T. I. Yacovitch, T. Wende, L. Jiang, N. Heine, G. Meijer, D. M. Neumark, K. R. Asmis, "Infrared Spectroscopy of Hydrated Bisulfate Anion Clusters: $HSO_4^-(H_2O)_{1–16}$", *Journal of Physical Chemistry Letter*, Vol. 2, Issue 17, pp. 2135−2140, 2011.

[16]. A. I. Boldyrev, J. Simons, "Isolated $SO_4^{2–}$ and $PO_4^{3–}$ Anions Do Not Exist", *Journal of Physical Chemistry*, Vol. 98, Issue 9, pp. 2298−2300, 1994.

[17]. A. B. Marahatta, "Theoretical Investigation of Electronic Structures and Stabilities of Microhydrated SO_4^{2-} and HSO_4^- Ions", *International Journal of Scientific Research in Multidisciplinary Studies*, Vol. 6, Issue 5, pp. 120−132, 2020.

[18]. A. B. Marahatta, "Chemical Energetics and Atomic Charges Distribution of Variably Sized Hydrated Sulfate Clusters in the light of Density Functional Theory", *International Journal of Progressive Sciences and Technologies*, Vol. 25, Issue 1, pp. 595−604, 2021.

[19]. A. B. Marahatta, "A DFT Study of Electronic Structures on Hydrated Sulfate Clusters $[SO_4^{2-}(H2O)n]$ n = 0−4, 16", *International Journal of Progressive Sciences and Technologies*, Vol. 17, Issue 1, pp. 55−69, 2019.

[20]. A. B. Marahatta, "Theoretical Study on Microhydration of Bisulfate Ions $[HSO_4(H_2O)_n]$ n = 0 − 3, 5", *International Journal of Progressive Sciences and Technologies*, Vol. 18, Issue 2, pp. 43−53, 2020.

[21]. A. B. Marahatta, "The QSPR Studies of $[SO_4 (H_2O)n]^{2-}$, n = 1−4, 16 Clusters through Quantum −Chemical Descriptors", *International Journal of Progressive Sciences and Technologies*, Vol. 27, Issue 2, pp. 441−454, 2021.

[22]. A. B. Marahatta, "Quantum Mechanical Viewpoint on Structural Stability of the Smallest Hydrated Sulfate Cluster $[SO_4(H_2O)_3]^{2-}$", International *Journal of Progressive Sciences and Technologies*, Vol. 28, Issue 2, pp. 572−583, 2021.

[23]. A. B. Marahatta, "Energy, Electronic, and Reactivity Descriptors in Quantitative Structure Property Relationships of $[HSO_4(H_2O)n]^-$, n = 0, 3, 4", *Chemistry Research Journal*, Vol. 7, Issue 2, pp. 56−69, 2022.

[24]. J. Curtius, E. R. Lovejoy, K. D. Froyd, "Atmospheric Ion-induced Aerosol Nucleation", *Space Science Reviews*, Vol. 125, pp. 159−167, 2006.

[25]. T. Kurten, M. Noppel, H. Vehkamaki, M. Salonen, M. Kulmala, "Quantum chemical studies of hydrate formation of H_2SO_4 and HSO_4^- ", *Boreal Environment Research*, Vol. 12, pp. 431−453, 2007.

[26]. F. Jensen, *Introduction to Computational Chemistry*, John Wiley & Sons, Chichester, 2003.

[27]. W. L. Jolly, *Modern Inorganic Chemistry, McGraw-Hill Book Company, New York, 1984.*

[28]. F. Jensen, *Introduction to Computational Chemistry*, John Wiley & Sons, Chichester, 2003.

[29]. C. F. Matta, R. J. Gillespie, "Understanding and Interpreting Molecular Electron Density Distributions", *Journal of Chemical Education*, Vol. 79, No. 9, pp. 1141−1152, 2002.

[30]. A. T. Blades, P. Kebarle, "Study of the Stability and Hydration of Doubly Charged Ions in the Gas Phase: SO_4^{2-}, $S_2O_6^{2-}$, $S_2O_8^{2-}$, and Some Related Species", *Journal of American Chemical Society*, Vol. 116, No. 23, pp. 10761−10766, 1994.

[31]. P. A. Hunt, B. Kirchner, T. Welton, "Characterizing the Electronic Structure of Ionic Liquids; An examination of the 1-Butyl-3-Methylimidazolium Chloride Ion Pair", *European Journal of Chemistry*, Vol. 12, Issue 26, pp. 6762−6775, 2006.

[32]. R. S. Mulliken, "Electronic Population Analysis on LCAO-MO Molecular Wave Functions", *The Journal of Chemical Physics*, Vol. 23, pp. 1833−1840, 1955.

[33]. C. F. Ding, X. B. Wang, L. S. Wang, "Photodetachment photoelectron spectroscopy of doubly charged anions: $S_2O_8^{2-}$", *Journal of Chemical Physics*, Vol. 110, Issue 8, pp. 3635−3638, 1999.

[34]. J. B. Foresman, Æ Frisch, *Exploring Chemistry with Electronic Structure Methods*, Gaussian, Inc.: Wallingford, CT, 2015.

[35]. P. Hohenberg, W. Kohn, "Inhomogeneous Electron Gas", *Physical Review B*, Vol. 136(3B), pp. 864−871, 1964.

[36]. Æ. Frisch, H. P. Hratchian, R. D. Dennington II, T. A. Keith, J. Millam, *Gauss view 05 Reference*, Gaussian, Inc.: Wallingford, CT, 2009.

[37]. A. B. Nadykto, F. Q. Yu, J. Herb, "Theoretical Analysis of the Gas-Phase Hydration of Common Atmospheric Pre-Nucleation $(HSO_4^-)(H_2O)n$ and $(H_3O^+)(H_2SO_4)(H_2O)_n$ Cluster Ions", *Chemical Physics*, Vol. 360, pp. 67–73, 2009.

[38]. M. J. Frisch, G. W. Trucks, H. B. Schlegel, G. E. Scuseria, M. A. Robb, J. R. Cheeseman, G. Scalmani, V. Barone, B. Mennucci, G. A. Petersson, *et al. Gaussian* 09, revision C.01; Gaussian, Inc.: Wallingford, CT, 2010.

[39]. Gaussian 09 manual. *http://gaussian.com/geom/?tabid=1#GeomkeywordReadOptimizeoption*

[40]. Æ. Frisch, *Gaussian 09W Reference*, Gaussian, Inc.: Wallingford, CT, 2009.

[41]. J. Rigby, E. I. Izgorodina, "Assessment of atomic partial charge schemes for polarisation and charge transfer effects in ionic liquids", *Physical Chemistry Chemical Physics*, Vol. 15, pp. 1632−1646, 2013.

[42]. G. V. Gibbs, A. F. Wallace, D. F. Cox, R. Downs, N. L. Ross, K. M. Rosso, "Bonded interactions in silica polymorphs, silicates, and siloxane molecules", *American Mineralogist* Vol. 94, pp. 1085−1102, 2009.

[43]. M. Fugel, J. Beckmann, D. Jayatilaka, G. V. Gibbs, S. Grabowsky, "A variety of bond analysis methods, one answer? An investigation of the element-oxygen bond of hydroxides H_nXOH", *European Journal of Chemistry*, Vol. 24, pp. 6248−6261, 2018.

[44]. L. Pauling, "The nature of the chemical bond", *Journal of Chemical Educ*ation, Vol. 69, pp. 519−522, 1992.

[45]. A. Krapp, G. Frenking, "Unicorns in the World of Chemical Bonding Models", *Journal of Computational Chemistry*, Vol. 28, No. 1, pp. 15−24, 2007.

[46]. G. D. Purvis, "On the use of isovalued surfaces to determine molecule shape and reaction pathways", *Journal of Computer-Aided Molecular Design*, Vol. 5, pp. 55−80, 1991.

[47]. A. C. Wahl, "Molecular Orbital Densities: Pictorial Studies", *Current Problems in Research*, pp 961−964, 1966.

[48]. B. T. Thole, P. Th. van Duijnen, "A general population analysis preserving the dipole moment", *Theoretica Chimica Acta*, Vol. 63, pp. 209–221, 1983.

[49]. C. M. Breneman, K. B. Wiberg "Determining atom-centered monopoles from molecular electrostatic potentials. The need for high sampling density in formamide conformational analysis", *Journal of Computational Chemistry, Vol.* 11, pp. 361−373, 1990.

[50]. Q-CHEM: A Quantum Leap Into the Future of Chemistry *https://manual.q-chem.com/5.3 /subsec_pop_anal.html*

[51]. ADF Manual 2022.1, *https://www.scm.com/doc/ADF/index.html*

[52]. Advanced charge density and bond order analysis, *https://www.scm.com/doc/ADF/Input/ Advanced_analysis.html*